Annealing Effects on the Structural and Optical Properties of Thermally Deposited Tin Antimony Sulfide Thin Films

Article *in* Brazilian Journal of Physics · December 2014

DOI: 10.1007/s13538-014-0255-1

CITATIONS
2

READS
94

8 authors, including:

Nisar Ali
GPG Jehanzeb College Mingora, Swat, Pakist…
49 PUBLICATIONS **280** CITATIONS
SEE PROFILE

Amiruddin Shaari
Universiti Teknologi Malaysia
59 PUBLICATIONS **277** CITATIONS
SEE PROFILE

Nisar Ahmad
45 PUBLICATIONS **213** CITATIONS
SEE PROFILE

Syed Mustansar Abbas
Dongguk University
44 PUBLICATIONS **248** CITATIONS
SEE PROFILE

Some of the authors of this publication are also working on these related projects:

Thin Film Solar Cells View project

properties of graphene thin films View project

Braz J Phys
DOI 10.1007/s13538-014-0255-1

Annealing Effects on the Structural and Optical Properties of Thermally Deposited Tin Antimony Sulfide Thin Films

N. Ali · R. Ahmed · A. Shaari · I. Rahim · M. Shah · A. Hussain · N. Ahmad · S. M. Abbas

Received: 1 May 2014 /

Abstract We report the deposition and characterization of tin antimony sulfide thin films on a soda glass substrate by a thermal evaporation technique. The thin films were annealed in argon gas at 150, 175, and 300 °C inside glass ampoules. The structural and optical properties of the deposited and annealed films are investigated. X-ray diffraction (XRD) patterns show that the films are polycrystalline in structure. Photoconductivity plot revealed good response in the NIR and visible regions, while the films show no transmittance below 700 nm. The absorption coefficient was of the order of 10^6 cm^{-1}. Optical band gaps were also evaluated and a decrease in band gap was observed due to annealing. Hot point probe technique was employed for type of conductivity.

Keywords Annealing · Solar cell · Transmittance · Absorption coefficient · XRD

1 Introduction

Photovoltaic is one of the fastest emerging industries with about 40 % annual growth. In the year 2008–2009, the researchers were stressed to work out alternative energy resources due to rapid increase in the cost of fossil energy resources. Under these circumstances, solar energy has naturally the best preference in energy conversion. The most capable solar cell devices were made from crystalline silicon. However, thin film technology made an interesting advent in photovoltaics with 10 % growth rate in the year 2009 [1]. Semiconductor materials are widely used for the fabrication of the solar cell devices [2]. Silicon is definitely not a good option for thin films due to a lot of constraints during its processing such as high temperatures and ultra-high vacuum production [1]. CdTe and $CuInGaSe_2$ (CIGS) are the most common thin film materials that have been used recently. They have produced devices with 10 % conversion efficiency; however, these are not acceptable by the researchers and the environmentalists due to the toxic behavior of cadmium. Moreover, gallium and indium are expensive and rare materials [1–3]. Metal chalcogenides can possibly fill up all the above mentioned deficiencies.

$SnSb_2S_4$ is a sulfosalt material with a band gap of about 1 eV, which is near the optimum value of 1.5 eV [3, 4] and possesses a very high absorption coefficient of 10^4 cm^{-1} [5]. These qualities make this material suitable as a new absorber layer for solar cell applications. The proposed material contains three elements Sn, Sb, and S. Fortunately, all the three are nontoxic and do not cause any harmful effect on the environment [3]. The present work deals with the study of the effect of annealing temperature on the structural and optical properties of thermally deposited tin antimony sulfide ($SnSb_2S_4$) thin films.

2 Materials and Methodology

Tin antimony sulfide ($SnSb_2S_4$) thin films were deposited on soda lime glass substrate using SnS and Sb_2S_3 by means of a

N. Ali · R. Ahmed · A. Shaari
Department of Physics, Faculty of Science, University Teknologi Malaysia, Skudai, Johor, Malaysia

N. Ali (✉) · N. Ahmad · S. M. Abbas
National Centre for Physics Islamabad, 2141, QAU Campus, Shahdra Valley Road, Islamabad 44000, Pakistan
e-mail: nisaraliswati@hotmail.com

N. Ali
e-mail: nisar.ali@utm.my

I. Rahim · M. Shah · A. Hussain
Institute of Physics and Electronics, University of Peshawar, Khyber, Pukhtunkhwa, Pakistan

Published online: 22 August 2014

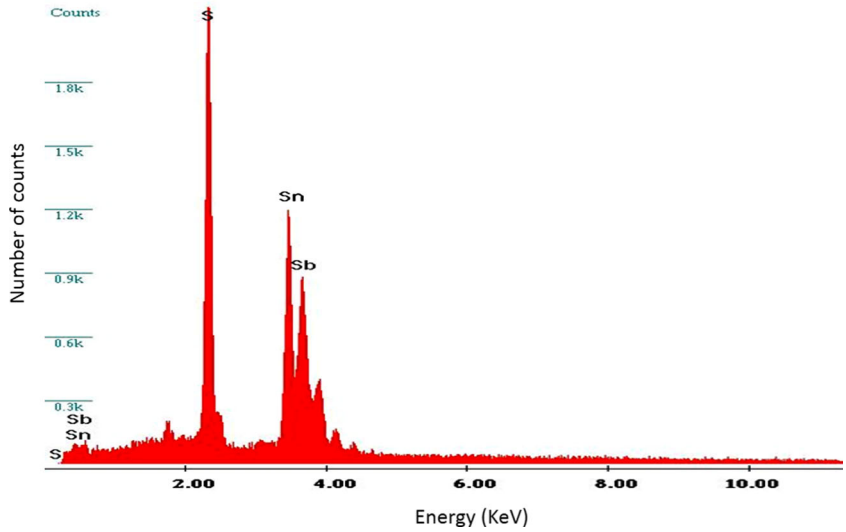

Fig. 1 EDX spectrum of the deposited thin film

two-source thermal evaporation method. Sb_2S_3 used in the experiment was of analytical grade with 99.99 % purity and obtained from Sigma-Aldrich. SnS was obtained from the tin and sulfur (powders) under the following scheme [6, 7]. Sn and S, 0.7873 and 0.2127 g, respectively, were mixed in pestle and mortar and annealed in quartz ampoule containing argon gas for 24 h at 600 °C. Both the powders, Sb_2S_3 and SnS, were mixed and evaporated from aluminum oxide crucibles via resistive basket simultaneously in a vacuum chamber. The pressure for the process was maintained approximately at 2×10^{-5} mbar. The films were annealed in argon atmosphere at 150, 175, and 300 °C. The films were characterized and their properties were analyzed [8, 9].

The structural and compositional properties of the thin films were determined by X-ray diffraction (XRD) patterns using the Cu Kα line (λ=0.15418 nm). The atomic composition of the elements was confirmed by energy dispersive X-ray spectroscopy (EDX). A spectrophotometer was used to measure the photoconductivity of the prepared thin film. The films were energized with light of variable wavelength ranging from 300 to 1,100 nm in the dark, and the response of the photoconductivity has been measured. The optical properties including energy band gap, thickness, absorption coefficient, transmittance, and refractive index were investigated by using J. A. Woollam variable angle ellipsometry (VASE). Hot point probe method measurements were carried out to find the type of conductivity of the proposed material [10, 11].

Table 1 Elemental composition of deposited Sn-Sb-S compound (atomic percentage)

S	Sn	Sb
52.11	37.44	10.46

3 Results and Discussions

Energy dispersive X-ray spectroscopy, Fig. 1, confirms the elemental compositions of the deposited films. Table 1 displays the compositions in terms of atomic percentage. The EDS study shows the $SbSn_{3.7}S_{5.2}$ composition of the deposited compound.

Figure 2 shows the XRD patterns of the material deposited as thin films. The figure reveals the structure of the deposited and the annealed films at various temperatures. The patterns contain resembling peaks with a major principal peak of $SnSb_2S_4$ at 2θ=32° [12]. These XRD patterns consist of two transition behaviors of polycrystalline nature liable to their annealing temperatures: (i) deposited film and (ii) films annealed till 300 °C. Other phases like Sb_2S_3 and SnS_2 are also expected to appear for this compound and usually appear at high annealing temperature (above 500 °C) [13, 14]. The XRD patterns indexed for different phases of SnS, and $SnSb_2S_4$ are shown in Fig. 2. The XRD results confirmed the phase $SnSb_2S_4$, since the range of annealing temperature is between 150–300 °C and the amorphous and other phases are expected at higher annealing temperature. Also, SnS_2 phases appear at low annealing temperature (100 °C and below) as well as in the deposited films [15]. In the deposited films, SnS, SnS_2, and at higher annealing

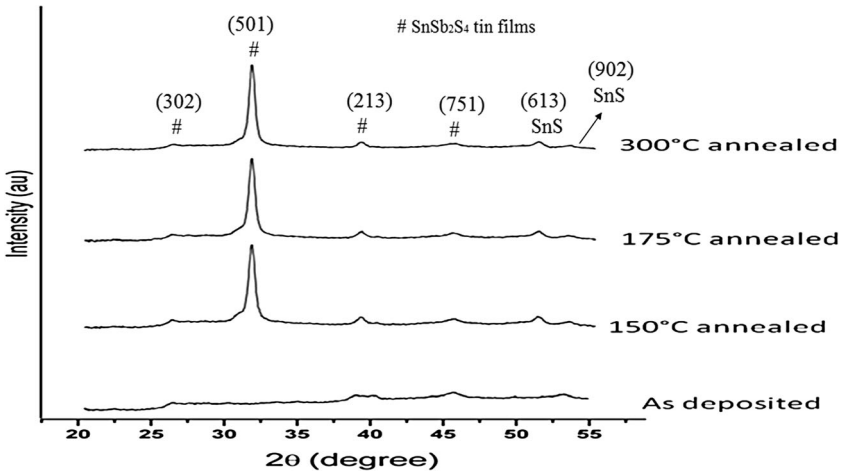

Fig. 2 X-ray diffraction spectrum of Sn-Sb-S in deposited and annealed films

temperature (up to 250 °C), few peaks of Sn_xS_y disappear [16, 17].

When the annealing temperature increases, the polycrystalline nature increases and the annealed films have good polycrystallinity. The grain size of the thin film was obtained by using Scherrer's formula [4, 18]:

$$D = \frac{0.9\lambda}{\beta\cos\theta} \quad . \tag{1}$$

Here, D is the grain size, λ is the wavelength of X-rays "Cu K_α radiation in angstroms," β is the full width at half maximum (FWHM), and θ is the Bragg angle. The "grain size D" of the 300 °C annealed film was found by using the principal peak of the material shown in the pattern and its average value was found to be 124 Å. The grain size increases from 74 Å for low-annealed samples.

The photoconductivity vs. wavelength for the deposited and annealed thin films is plotted and given in Fig. 3. The graph shows that the thin film annealed at 150 °C and above has better photoconductivity. It is observed that the photoconductivity of the films increases with the annealing temperature. This increase in photoconductivity is in optical spectral range as well as intensity. The annealed thin films have good response in the visible and NIR regions of the solar spectrum. The increase in photoconductivity is attributed to the increase in the crystallite size and reduction in impurities with annealing temperature. The increase in the annealing temperature increases the polycrystalline nature of the material and hence the increase in grain size. The 300 °C sample grain size is on the average 124 Å. This high value of grain increases the exciton transitions between the grains due to reduction in impurities as well as compactness of the material. These phenomena are responsible for the increase in photoconductivity of the thin films.

The transmittance plots of the thin films in the wavelength range 200–1,800 nm are shown in Fig. 4. The transmittance is almost negligible till 700 nm; after that, it rises sharply due to high absorption power of antimony. The high absorbance in the visible-NIR region makes the material useful for p-n junction formation solar cells and suitable materials for photovoltaic applications. We noted that the transmittances of the thin films decreased with the increasing annealing temperature. The films annealed at 300 °C have the lowest transmittance. The optical

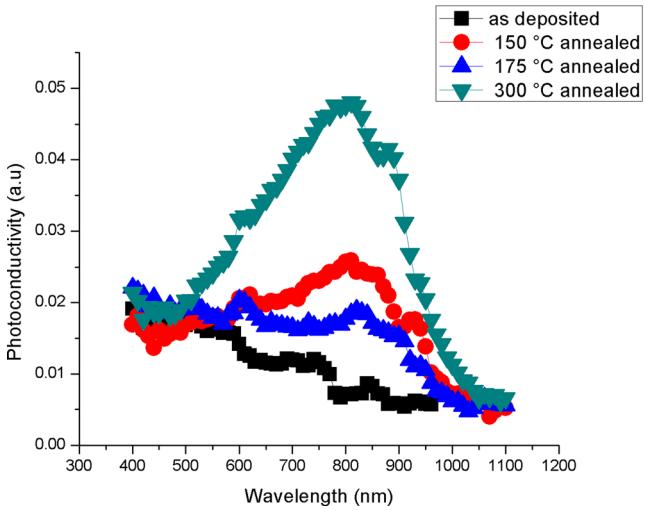

Fig. 3 Photoconductivity response of the as-deposited and annealed films grown on soda lime glass substrate

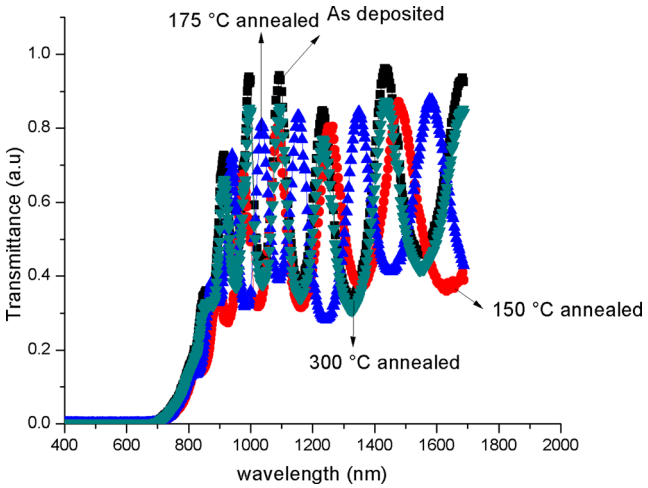

Fig. 4 Transmittance of $SnSb_2S_4$ as-deposited and annealed thin films

spectrum of the transmittance as presented (Fig. 4) shows that the film transmits well above the visible region of the spectrum and tends to be constant in the far infrared region. The 300 °C annealed film is polycrystalline in nature, and the grain size is maximum which helps in reduction of the irradiance. SnS is volatile and it not only deteriorates the structure but also reduces the content of Sn in the compound. This leads to an increase in the content of Sb in the compound (Sn-Sb-S). Sb-rich compound reduces the transmittance as reported earlier [19].

The plot of absorption coefficient α versus wavelength λ for as-deposited and the annealed thin films of the proposed material are shown in Fig. 5. The absorption coefficient was calculated using the extinction coefficient and wavelength obtained from the ellipsometric modeled data and fitted for suitable model (B-spline layer) shown in Fig. 6. We used J.A Woolam Ellipsometry to calculate the function (Ψ) containing all the information including refractive index, extinction coefficient, thickness etc. for each wavelength (300–1,200 nm). The model was fitted on B-spline layer.

When the raw ellipsometric data is modeled on B-spline layer, we export an excel file containing the values of n and k for each wavelength (ranging from 300–1,200 nm).

The extinction coefficient "k" and absorption coefficient "α" can be related as [20]

$$\alpha = 4\pi k/\lambda \ .$$

The modeled data resulted in thickness of the order of 2 μm and the average refractive index of 3.0. The absorption edge lies approximately at 700 nm. The material shows high absorbance in the NIR and visible regions of the solar spectrum making our material suitable for solar cell application. The absorption coefficient of the material is in the range of 4×10^5 to 8.5×10^5 cm^{-1}, thus characterizing our material as a potential material to be used as an absorber layer in solar cell.

The prepared thin films show increasing trends in absorbance with the increase in annealing temperature. This is due to increase in grain size, oxygen deficiency, and the reduced number of defects in the annealed samples [21, 22].

The optical band gap of the films was calculated as in reference [23] and shown in Fig. 7. The linear nature of the plot indicates the existence of the direct transition [24]. The band gap of the deposited film is 2.66 eV whereas the band gap of the annealed films at 150 and 175 °C is

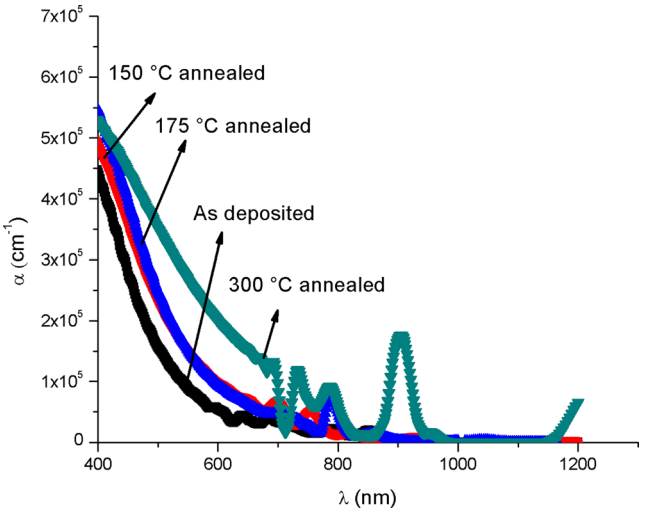

Fig. 5 Absorption coefficient α of $SnSb_2S_4$ as-deposited and annealed samples

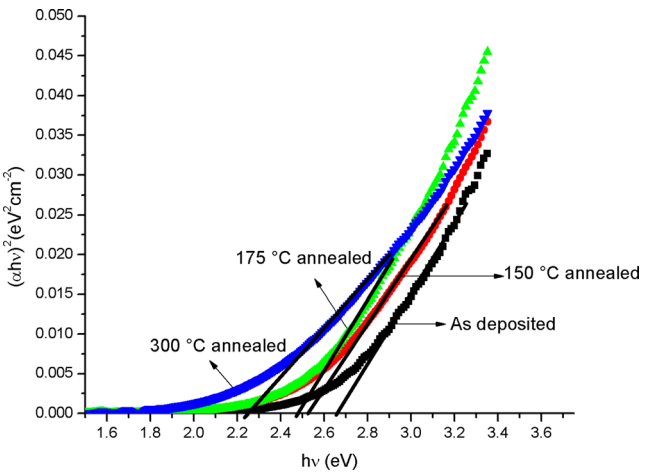

Fig. 6 Modeled data of experimental curve for calculating n and k using B-spline layer model

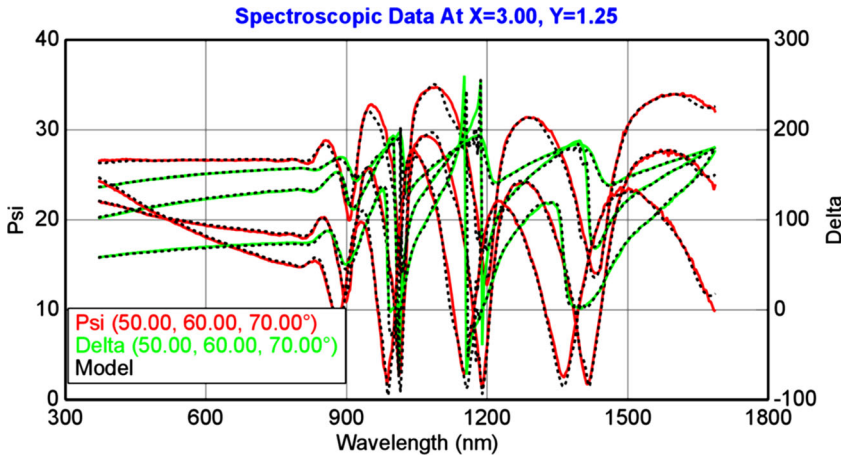

Fig. 7 Band gap of the as-deposited and annealed films at 150, 175, and 300 °C

reduced to 2.55 eV and 2.45 eV, respectively. Film annealed at 300 °C shows much more suitable band gap of 2.25 eV as compared to that of the films annealed at lower temperatures. The decrease of the band gap is due to increase in the crystal size with annealing [26]. However, antimony is also responsible for this decreasing trend as it makes the films good absorbents by decreasing the transmittance of the crystalline films [25].

The type of the conductivity of the films was tested by hot point probe method. Molybdenum contacts were sputtered on the films and produce a temperature difference between the contacts with the help of solder ion.

The thermal Seebeck effect creates potential difference between hot and cold contacts, and the carrier type is identified by the deflection of central-zero meter. The free carrier diffuses more rapidly near the hot end leading current away from the hot contact and vice versa. The directions of electric current (toward or away the hot contact) identify the type of conductivity [25, 26]. In this study, the instrument was calibrated for *n*-type silicon wafer and then the conductivity type of thin films was measured. The conductivity type of $SnSb_2S_4$ was calculated and was found that the deposited and annealed films both show *n*-type conductivity as given in Fig. 8.

4 Conclusion

Fine-quality tin antimony sulfide ($SnSb_2S_4$) thin films were prepared by a thermal evaporation technique. The annealing effect of inert atmosphere on the films has been studied and analyzed. The annealing process has been noted to be helpful in improving the electro-optical properties of thin film. This may be due to a better crystalline quality and oxygen deficiency after annealing.

The films were polycrystalline in nature as confirmed from the XRD patterns. The as-deposited and low-temperature annealed films have shown poor photoconductivity response; however, this response increases with high annealing temperature covering NIR and visible part of the solar spectrum. There is no transmittance below 700 nm due to opaqueness of antimony metal present in the compound. The absorption coefficient was of the order 8×10^5 cm^{-1}. The material exhibited a direct band gap of 2.66 eV for the deposited and 2.25–2.45 eV for the annealed films, respectively.

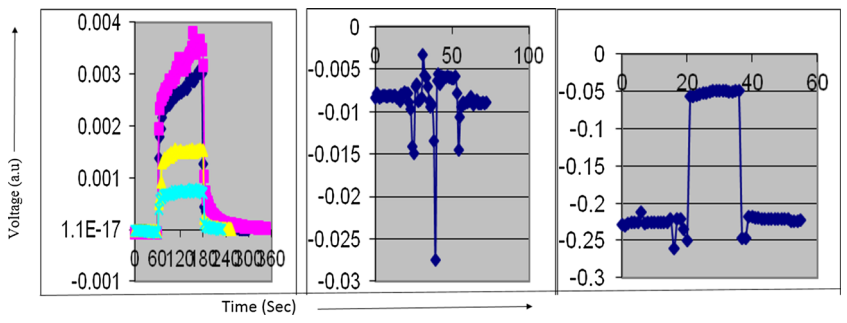

Fig. 8 Hot point probe calculation for the conductivity of Sn-Sb-S thin films

Acknowledgement The authors would like to thank University Teknologi Malaysia for the financial support of this research work through Post-Doctoral Fellowship Scheme.

References

1. A. Bosio, D. Menossi, S. Mazzamuto, N. Romeo, Manufacturing of CdTe thin film photovoltaic modules. J Thin Solid Films **519**, 7522–7525 (2011)
2. S. Kumara, T.P. Sharma, M. Zulfequar, M. Husain, Characterization of vacuum evaporated PbS thin films. J Physica B **325**, 8–16 (2003)
3. S. Cheng, G. Conibeer, Physical properties of very thin SnS films deposited by thermal evaporation. J. Thin Solid Films **520**, 837–841 (2011)
4. A. Gassoumi, M. Kanzari, Effect of growth conditions on the physical properties of the sulfosalt $SnSb_2S_4$ thin films deposited by the thermal vacuum evaporation technique. J J Optoelectron Adv Mater **14**, 272–276 (2012)
5. H. Dittrich, A. Bieniok, U. Brendel, M. Grodzicki, D. Topa, Sulfosalts—a new class of compound semiconductors for photovoltaic applications. J. Thin Solid Films. **515**, 5745–5750 (2007)
6. Massalski, T.B.; Okamoto, H; ASM international, Technology and Engineering v. 2, 1990.
7. C. Cifuentes, M. Botero, E. Romero, C. Calderón, G. Gordillo, Optical and structural studies on SnS films grown by co-evaporation. Braz J Phys **36**, 1046–1049 (2006)
8. W. Vallejo, J. Clavijo, G. Gordillo, CGS based solar cells with In2S3 buffer layer deposited by CBD and coevaporation. Braz J Phys **40**, 30–37 (2010)
9. L. Tirado-Mejía, J.G. Ramírez, M.E. Gómez, H. Ariza-Calderón, Surface morphology analysis of GaInAsSb films grown by liquid phase epitaxy. Braz J Phys **36**, 1070–1073 (2006)
10. B. Johs, J.S. Hale, Dielectric function representation by B-splines. Physica Status Solidi (a). **205**, 715–9 (2008)
11. R.A. Synowicki, B.D. Johs, A.C. Martin, Optical properties of soda-lime float glass from spectroscopic ellipsometry. Thin Solid Films **519**, 2907–2913 (2011)
12. N. Ali, S.T. Hussain, K. Yaqoob, A. Nisar, M.A. Iqbal, S.M. Abbas, Effect of air annealing on the band gap and optical properties of SnSb2S4 thin films for solar cell application. Mater Lett **100**, 148 (2013)
13. B. Krishnan, A. Arato, E. Cardenas, T.K. Das Roy, G.A. Castillo, On the structure, morphology, and optical properties of chemical bath deposited Sb_2S_3 thin films. J. Applied Surface Science **254**(10), 3200–3206 (2008)
14. Sousa, M. G.; A. Da Cunha A. F.; Fernandes P. A. J. Alloys and Compounds 014, 592, 80–85.
15. M. Patel, I. Mukhopadhyay, A. Ray, Annealing influence over structural and optical properties of sprayed SnS thin films. Opt Mater **35**, 1693–1699 (2013)
16. G.H. Yue, W. Wang, L.S. Wang, X. Wang, P.X. Yan, Y. Chen et al., The effect of anneal temperature on physical properties of SnS films. J Alloys Compd **474**, 445–449 (2009)
17. N.R. Mathews, C. Colín García, I.Z. Torres, Effect of annealing on structural, optical and electrical properties of pulse electrodeposited tin sulfide films. Mater Sci Semicond Process **16**, 29–37 (2013)
18. S.F. Bartram, in *Handbook of X-rays*, ed. by E.F. Kaelebe (McGraw-Hill, New York, 1967)
19. J. Ge, Y. Wu, C. Zhang, S. Zuo, J. Jiang, J. Ma et al., Comparative study of the influence of two distinct sulfurization ramping rates on the properties of Cu2ZnSnS4 thin films. Appl Surf Sci **258**, 7250–7254 (2012)
20. Tompkins, H., and Irene, E. A. Handbook of Ellipsometry, Elsevier Science, 2005
21. F.I. Ezema, A.B..C. Ekwealor, R.U. Osuji, Effect of thermal annealing on the band Gap and optical properties of chemical bath deposited ZnSe thin films J. Turk J Phys **30**, 157–163 (2006)
22. P.E. Agbo, Effect of thermal annealing on optical and band gap of chemically deposited TiO_2/Fe_2O_3 core/shell oxide thin films. J. Adv ApplSci Res **2**(6), 393–399 (2011)
23. N. Ali, S.A.T. Hussain, M.A. Iqbal, K. Hutching, D. Lane, Structural and optoelectronic properties of antimony tin sulphide thin films deposited by thermal evaporation techniques. Optik. Int J Light and Electron Optics **124**(21), 4746 (2013)
24. A. Gassoumi, M. Kanzari, B. Rezig, Thermally induced changes in optical and electrical properties of $SnSb_2S_4$ thin films. Eur Phys J Appl Phys **41**(2), 91–95 (2008)
25. Plummer, J. D.; Deal, M. D.; Grsffin, P. B.; Silicon VLSI Technology. Fundamentals, Practice and Modeling: Dorling Kindersley Publishers, 2009c
26. N. Ali, S.T. Hussain, M.A. Iqbal, Z. Iqbal, D. Lane, Metal based chalcogenide thin films for photovoltaics. Chalcogenide Lett **9**(11), 435 (2012)